Acta Crystallographica Section F
Structural Biology and Crystallization Communications
ISSN 1744-3091

Crystallization and preliminary X-ray diffraction studies of a novel ferredoxin involved in the dioxygenation of carbazole by *Novosphingobium* sp. KA1

Takashi Umeda,[a] Junichi Katsuki,[a] Yusuke Usami,[a] Kengo Inoue,[a] Haruko Noguchi,[a] Zui Fujimoto,[b] Yuji Ashikawa,[c] Hisakazu Yamane[a] and Hideaki Nojiri[a,d]*

[a]Biotechnology Research Center, University of Tokyo, 1-1-1 Yayoi, Bunkyo-ku, Tokyo 113-8657, Japan, [b]Protein Research Unit, National Institute of Agrobiological Sciences, 2-1-2 Kannondai, Tsukuba, Ibaraki 305-8602, Japan, [c]Molecular Signaling Research Team, Structural Physiology Research Group, RIKEN Harima Institute SPring-8 Center, 1-1-1 Kouto, Sayo, Hyogo 679-5148, Japan, and [d]Professional Programme for Agricultural Bioinformatics, University of Tokyo, 1-1-1 Yayoi, Bunkyo-ku, Tokyo 113-8657, Japan

Correspondence e-mail: anojiri@mail.ecc.u-tokyo.ac.jp

Received 4 April 2008
Accepted 29 May 2008

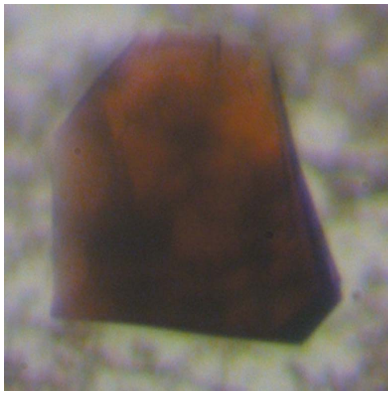

Novosphingobium sp. KA1 uses carbazole 1,9a-dioxygenase (CARDO) as the first dioxygenase in its carbazole-degradation pathway. The CARDO of KA1 contains a terminal oxygenase component and two electron-transfer components: ferredoxin and ferredoxin reductase. In contrast to the CARDO systems of other species, the ferredoxin component of KA1 is a putidaredoxin-type protein. This novel ferredoxin was crystallized at 293 K by the hanging-drop vapour-diffusion method using PEG MME 550 as the precipitant under anaerobic conditions. The crystals belong to space group $C222_1$ and diffraction data were collected to a resolution of 1.9 Å (the diffraction limit was 1.6 Å).

1. Introduction

[2Fe–2S]-type ferredoxins are small iron–sulfur proteins that are found in bacteria, plants and animals, where they participate in a wide variety of electron-transfer reactions. In chloroplast-type ferredoxins, which were the first electron-transfer proteins to be identified in the plant photosystem, the [2Fe–2S] cluster is ligated by four cysteinyl residues that are bound to both of the Fe atoms (Tagawa & Arnon, 1962). In contrast, Rieske-type ferredoxins, which were first isolated from the cytochrome *c* reductase complex in bovine heart mitochondria, consist of a [2Fe–2S] core with two histidine side chains bound to one Fe atom and two cysteine side chains bound to the other (Rieske *et al.*, 1964). Although the [2Fe–2S] cluster in putidaredoxin-type ferredoxins is ligated by four cysteinyl residues, as in chloroplast-type ferredoxins, they are frequently involved in oxidation reactions, such as those of the P450 monooxygenase system in bacteria (Hannemann *et al.*, 2007).

Rieske nonhaem iron-oxygenase systems (ROSs) are the primary catalysts in the bacterial aerobic degradation of many environmentally significant aromatic compounds, including polycyclic aromatic hydrocarbons, polychlorinated biphenyl and heteroaromatics such as dioxins and carbazole (Nojiri & Omori, 2002; Habe & Omori, 2003; Furukawa *et al.*, 2004; Pieper, 2005). ROSs consist of a terminal oxygenase component and either a single reductase component or ferredoxin and ferredoxin reductase components, which are involved in the transfer of electrons from NAD(P)H to the terminal oxygenase. ROSs are divided into five groups (IA, IB, IIA, IIB and III) based on the number of constituents they contain and the nature of their redox centres. The three-component systems are further classified as IIA, IIB or III (Batie *et al.*, 1991). Many ROS members that belong to Batie classes IIB or III contain a Rieske-type ferredoxin that mediates the movement of electrons from the reductase to the terminal oxygenase component. To elucidate the function of Rieske-type ferredoxins in ROS catalysis, the crystal structures and biological functions of several Rieske-type ferredoxins have been analysed (Colbert *et al.*, 2000; Nam *et al.*, 2005; Ferraro *et al.*, 2007). In contrast, a few ROSs belong to class IIA, in which a putidaredoxin-type ferredoxin mediates the movement of electrons between the reductase and terminal oxygenase components (Sauber *et al.*, 1977; Bünz & Cook, 1993; Herman *et al.*, 2005).

Novosphingobium sp. KA1 (formerly *Sphingomonas* sp. KA1) possesses the carbazole-degradative plasmid pCAR3 (Shintani *et al.*,

2007), which carries several genes (*carAaIAcIAdI*, *carAaIIAcIIAdII*, *fdxI* and *fdrI*/*fdrII*) that are involved in the conversion of carbazole to anthranilate (Urata *et al.*, 2006). The initial dioxygenation of carbazole is catalysed by carbazole 1,9a-dioxygenase (CARDO; Fig. 1), which consists of three components: the terminal oxygenase CARDO-O (CarAaI or CarAaII), the ferredoxin CARDO-F (CarAcI, CarAcII or FdxI) and the ferredoxin reductase CARDO-R (FdrI or FdrII) (Urata *et al.*, 2006). The CARDO-F of *Novosphingobium* sp. KA1 (CARDO-F_{KA1}) is a putidaredoxin-type ferredoxin, while CARDO-R shows marked homology to the putidaredoxin reductase involved in camphor oxidation by the cytochrome P450 monooxygenase of *Pseudomonas putida* (Poulos, 2003). Thus, the CARDO of *Novosphingobium* sp. KA1 ($CARDO_{KA1}$) belongs to class IIA. We have previously investigated the structures and functions of the CARDOs from several bacterial strains, including *P. resinovorans* CA10, *Janthinobacterium* sp. J3 and *Nocardioides aromaticivorans* IC177, which belong to classes III, III and IIB, respectively (Nojiri & Omori, 2007). The CARDO-Os of many species are coupled with diverse types of electron-transfer components, although they share marked homology (>45% identity and >70% similarity at the primary sequence level) to each other. Therefore, CARDOs are an excellent model for studying the molecular mechanism of electron transfer between the terminal oxygenase and ferredoxin components, which has been largely overlooked compared with that between reductase and ferredoxin components (Senda *et al.*, 2007). To date, we have determined the crystal structures of the components of a class III CARDO, CARDO-F of *P. resinovorans* CA10 (Nam *et al.*, 2005), CARDO-O of *Janthinobacterium* sp. J3 (Nojiri *et al.*, 2005) and their electron-transfer complex (Ashikawa *et al.*, 2005, 2006). We have also successfully crystallized a class IIB CARDO-O and CARDO-F from *N. aromaticivorans* (Inoue *et al.*, 2006, 2007) and we recently finalized the structures of both components at resolutions of 2.3 and 2.0 Å, respectively (Inoue *et al.*, unpublished results). Crystal structures of components of class IIA ROSs such as $CARDO_{KA1}$ have not been reported; however, the crystal structures of homologous ferredoxins, including bovine adrenodoxin (Pikuleva *et al.*, 2000), multiple putidaredoxin mutants (Sevrioukova *et al.*, 2003; Smith *et al.*, 2004) and a ferredoxin from *Rhodobacter capsulatus* (Sainz *et al.*, 2006), have been determined.

Here, we report the crystallization and preliminary X-ray diffraction of class IIA CARDO-F_{KA1} (109 residues with a molecular mass of 11.5 kDa). The three-dimensional structure of CARDO-F_{KA1} will provide meaningful insights into the mechanisms of electron transfer and recognition of the proper redox partner.

2. Experimental methods

2.1. Protein expression and purification

carAcII (the accession No. of the corresponding protein is YP_717946) was amplified by PCR using the primers 5′-AAAAA-ATCTAGAATAAGGAGGTGTT*CATATG***CACCACCACCACCA-CCAC**TCGGAGACCATCCGGCTC-3′ and 5′-AAAAAAGGTAC-C*AAGCTT*TCAGAGCTGACTGGCGGGCAG-3′ (the *Nde*I and *Hin*dIII restriction sites and 6×His-tag sequence are italicized and shown in bold, respectively) and the product was ligated into pUC119 (Sambrook & Russell, 2001). The insert was sequenced to verify its accuracy and the 350 bp *Nde*I–*Hin*dIII fragment was inserted into the expression vector pET-26b(+) (Novagen) to create pEKANhAcII, which encodes His-tagged CARDO-F_{KA1} in which a 6×His tag is inserted between the starting methionine and the following serine residues. Following overnight culture of *Escherichia coli* BL21 (DE3) (Novagen) cells carrying pEKANhAcII at 310 K in LB medium (Sambrook & Russell, 2001) supplemented with kanamycin (50 µg ml^{-1}), this culture was diluted 50-fold into SB medium (12 g tryptone, 24 g yeast extract, 5 ml glycerol, 12.5 g K_2HPO_4 and 3.8 g KH_2PO_4 per litre; Nam *et al.*, 2002) with kanamycin and cultivated at 298 K with shaking at 120 rev min^{-1}. When the optical density at 600 nm reached approximately 0.5, isopropyl *β*-D-1-thiogalactopyranoside was added to a final concentration of 0.5 m*M*. After a 15 h incubation, the cells were harvested by centrifugation at 5000*g* for 10 min, washed twice with TG buffer (20 m*M* Tris–HCl pH 7.5 and 10% glycerol; Nam *et al.*, 2002) and resuspended in buffer *A* (TG buffer containing 0.5 *M* NaCl and 10 m*M* imidazole). A crude cell extract was then prepared by sonication and centrifugation at 25 000*g* for 1 h and the supernatant was applied onto a HiTrap Chelating HP column (GE Healthcare) on an ÄKTA FPLC instrument (GE Healthcare) according to the manufacturer's recommendations. CARDO-F_{KA1} was eluted using a gradient of 10–200 m*M* imidazole in buffer *A*. The fractions containing CARDO-F_{KA1} were pooled and concentrated by ultrafiltration using Centriprep YM-10 columns (Millipore). The concentrated fraction was applied onto a Hi-Prep 16/10 DEAE (GE Healthcare) column equilibrated with TG buffer and eluted using a gradient of 0–1.0 *M* NaCl in TG buffer. The fractions containing CARDO-F_{KA1} were pooled and concentrated as

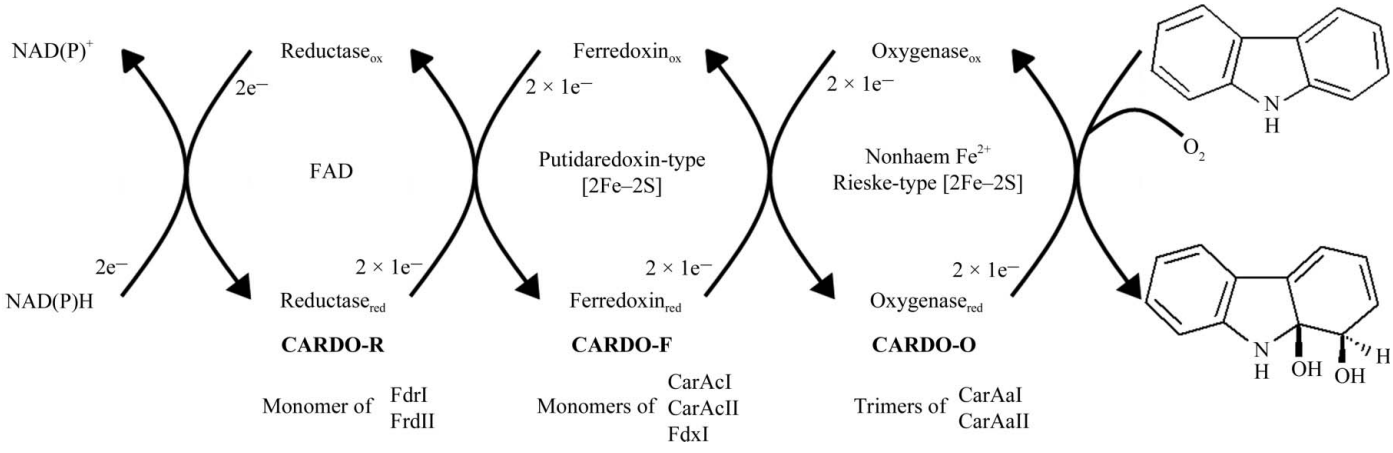

Figure 1
Components and functions of the class IIA CARDO system. The proposed electron-transfer and dioxygenation reactions are illustrated. The subscripts 'ox' and 'red' indicate the oxidized and reduced states of the CARDO components, respectively.

described above. The resultant preparation was further purified by gel-filtration chromatography using a Superdex75 prep-grade (GE Healthcare) column and GFC buffer (20 m*M* Tris–HCl buffer pH 7.5 containing 0.2 *M* NaCl and 10% glycerol; Nam *et al.*, 2002). The homogeneity of the purified CARDO-F_{KA1} (molecular mass of 12.5 kDa) was confirmed by SDS–PAGE. The amount of CARDO-F_{KA1} harvested was approximately 4 mg per litre of SB medium. Protein concentrations were estimated using a protein-assay kit (Bio-Rad) according to the method of Bradford (1976) with BSA as a standard. Prior to crystallization, the ability of the purified CARDO-F_{KA1} to transfer electrons from CARDO-R_{KA1} to CARDO-O_{KA1} was confirmed *in vitro* by the detection of oxygenation activity using carbazole (data not shown).

2.2. Crystallization

CARDO-F_{KA1} appeared to be unstable under aerobic conditions, given that the colour of the protein solution changed from dark brown to colourless. No putidaredoxins had been crystallized in recent years because of instability until Sevrioukova *et al.* (2003) reported the crystallization of putidaredoxin mutants with Ser residues substituted for several Cys residues located on the surface of the protein. Based on their data, the stabilization of CARDO-F_{KA1} under anaerobic conditions was presumed to be the consequence of a reduction in the auto-oxidation of Cys residues located on the surface of the protein. In fact, we found that under anaerobic conditions CARDO-F_{KA1} was stable in 5 m*M* Tris–HCl pH 7.5 for several weeks. Therefore, the crystallization of CARDO-F_{KA1} was performed in an anaerobic chamber (Te-Her Anaerobox ANX-3, Hirasawa) filled with 80% N_2, 10% CO_2 and 10% H_2. All remaining oxygen molecules in the chamber were removed using a Pd catalyst, which catalyses the conversion of H_2 to H_2O. The gas mixture was introduced for 2 min every 24 h in order to maintain anaerobic conditions. Anaerobic conditions were verified prior to the experiment using a BR0055B anaerobic indicator (Oxoid).

For crystallization, a solution of CARDO-F_{KA1} containing 5–20 mg ml^{-1} protein in 5 m*M* Tris–HCl pH 7.5 was used. Crystallization was performed by the hanging-drop vapour-diffusion method at 293 K. Drops containing 2 µl protein solution and 2 µl mother liquor were equilibrated against 500 µl reservoir solution. The initial crystallization conditions were screened using Crystal Screens I and II and Index Screen (Hampton Research). Several crystals were obtained using Index Screen condition No. 54 [0.05 *M* calcium chloride dihydrate, 0.1 *M* bis-tris pH 6.5 and 30%(*v*/*v*) polyethylene glycol monomethyl ether 550]. The crystals, which appeared within two weeks at a protein concentration of 5 mg ml^{-1}, grew to approximate dimensions of 0.25 × 0.2 × 0.05 mm (Fig. 2).

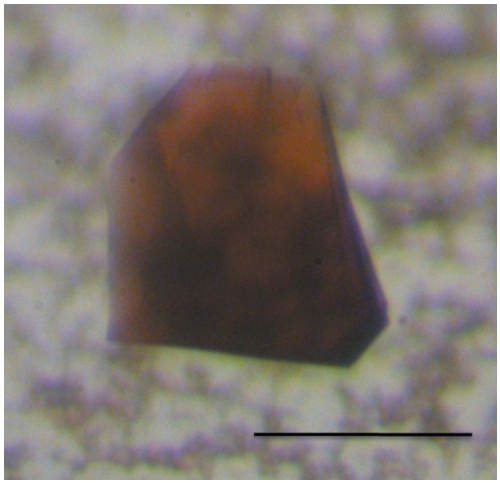

Figure 2
A CARDO-F_{KA1} crystal. The scale bar indicates 0.16 mm.

Table 1
Crystal parameters and data-collection statistics.

The data were collected on BL-6A at the Photon Factory in Tsukuba, Japan. Values in parentheses are for the highest resolution shell.

Wavelength (Å)	1.000
Space group	$C222_1$
Unit-cell parameters (Å, °)	a = 53.4, b = 77.8, c = 43.5, $\alpha = \beta = \gamma$ = 90
Resolution range (Å)	30.93–1.90 (1.95–1.90)
Diffraction limit (Å)	1.60
Total No. of reflections	50995
No. of unique reflections	7436 (715)
Completeness (%)	99.9 (100)
Average $I/\sigma(I)$	43.1 (7.3)
R_{merge}† (%)	6.5 (32.8)
Multiplicity	6.9 (6.9)

† $R_{merge} = \sum_{hkl}\sum_i |I_i(hkl) - \langle I(hkl)\rangle| / \sum_{hkl}\sum_i I_i(hkl)$, where $I_i(hkl)$ is the ith observation of reflection hkl and $\langle I(hkl)\rangle$ is the weighted average intensity for all observations of reflection hkl.

2.3. Data collection

The crystals were directly flash-cooled in a nitrogen stream at 100 K. Diffraction experiments were conducted on beamline BL-6A at Photon Factory, Tsukuba, Japan. The data were collected at a wavelength of 1.000 Å with a Quantum 4R CCD X-ray detector (ADSC) using a single crystal in 0.5° oscillation steps over a range of 180° with a 60 s exposure per frame. The crystals diffracted to a diffraction limit of 1.6 Å. The data sets were integrated and scaled using the *HKL*-2000 program suite (Otwinowski & Minor, 1997) to 1.9 Å resolution. The criterion for determination of the resolution range used was the resolution at which the R_{merge} remains less than 0.35. Our data-collection and processing statistics are summarized in Table 1.

3. Results and discussion

We have obtained crystals of CARDO-F_{KA1}. The space group of the crystal was determined to be $C222_1$, with unit-cell parameters a = 53.4, b = 77.8, c = 43.5 Å, $\alpha = \beta = \gamma = 90°$. Initial analysis of the crystal solvent content using the Matthews coefficient (Matthews, 1968) suggested that the asymmetric unit contained one molecule (33.0% solvent content) with an acceptable packing density V_M of 1.83 Å^3 Da^{-1}.

The crystal structure solution was attempted using molecular replacement with the solution structure of putidaredoxin (PDB code 1pdx; 45% primary sequence identity; Pochapsky *et al.*, 1999) as a search model and yielded a satisfactory solution. A full description of the structure determination followed by interpretation of the structure–function relationship will be published elsewhere.

This work was supported by a Grant-in-Aid for Scientific Research (17380052 to HN) from the Ministry of Education, Culture, Sports, Science and Technology of Japan and by the Institute for Bioinformatics Research Development, Japan Science Technology Agency (BIRD-JST). The use of synchrotron radiation was approved by the Photon Factory Advisory Committee and KEK (High-Energy

Accelerator Research Organization), Tsukuba (proposals 04G137, 2006G171 and 2007G135).

References

Ashikawa, Y., Fujimoto, Z., Noguchi, H., Habe, H., Omori, T., Yamane, H. & Nojiri, H. (2005). *Acta Cryst.* F**61**, 577–580.

Ashikawa, Y., Fujimoto, Z., Noguchi, H., Habe, H., Omori, T., Yamane, H. & Nojiri, H. (2006). *Structure*, **14**, 1779–1789.

Batie, C. J., Ballou, D. P. & Correll, C. C. (1991). *Chemistry and Biochemistry of Flavoenzymes*, Vol. 3, edited by F. Muller, pp. 543–556. Boca Raton: CRC Press.

Bradford, M. M. (1976). *Anal. Chem.* **72**, 248–254.

Bünz, P. V. & Cook, A. M. (1993). *J. Bacteriol.* **175**, 6467–6475.

Colbert, C. L., Couture, M. M., Eltis, L. D. & Bolin, J. T. (2000). *Structure*, **8**, 1267–1278.

Ferraro, D. J., Brown, E. N., Yu, C. L., Parales, R. E., Gibson, D. T. & Ramaswamy, S. (2007). *BMC Struct. Biol.* **7**, 10.

Furukawa, K., Suenaga, H. & Goto, M. (2004). *J. Bacteriol.* **186**, 5189–5196.

Habe, H. & Omori, T. (2003). *Biosci. Biotechnol. Biochem.* **67**, 225–243.

Hannemann, F., Bichet, A., Ewen, K. M. & Bernhardt, R. (2007). *Biochim. Biophys. Acta*, **1770**, 330–344.

Herman, P. L., Behrens, M., Chakraborty, S., Chrastil, B. M., Barycki, J. & Weeks, D. P. (2005). *J. Biol. Chem.* **280**, 24759–24767.

Inoue, K., Ashikawa, Y., Usami, Y., Noguchi, H., Fujimoto, Z., Yamane, H. & Nojiri, H. (2006). *Acta Cryst.* F**62**, 1212–1214.

Inoue, K., Ashikawa, Y., Usami, Y., Noguchi, H., Fujimoto, Z., Yamane, H. & Nojiri, H. (2007). *Acta Cryst.* F**63**, 855–857.

Matthews, B. W. (1968). *J. Mol. Biol.* **33**, 491–497.

Nam, J.-W., Noguchi, H., Fujimoto, Z., Mizuno, H., Ashikawa, Y., Abo, M., Fushinobu, S., Kobashi, K., Wakagi, T., Iwata, K., Yoshida, T., Habe, H., Yamane, H., Omori, T. & Nojiri, H. (2005). *Proteins*, **58**, 779–789.

Nam, J.-W., Nojiri, H., Noguchi, H., Uchimura, H., Yoshida, T., Habe, H., Yamane, H. & Omori, T. (2002). *Appl. Environ. Microbiol.* **68**, 5882–5890.

Nojiri, H., Ashikawa, Y., Noguchi, H., Nam, J.-W., Urata, M., Fujimoto, Z., Yoshida, T., Habe, H. & Omori, T. (2005). *J. Mol. Biol.* **351**, 355–370.

Nojiri, H. & Omori, T. (2002). *Biosci. Biotechnol. Biochem.* **66**, 2001–2016.

Nojiri, H. & Omori, T. (2007). *Pseudomonas*, Vol. 5, *A Model System in Biology*, edited by J. L. Ramos & A. Filloux, pp. 107–145. New York, USA: Kluwer Academic/Plenum Publishers.

Otwinowski, Z. & Minor, W. (1997). *Methods Enzymol.* **276**, 307–326.

Pieper, D. H. (2005). *Appl. Microbiol. Biotechnol.* **67**, 170–191.

Pikuleva, I. A., Tesh, K., Waterman, M. R. & Kim, Y. (2000). *Arch. Biochem. Biophys.* **373**, 44–55.

Pochapsky, T. C., Jain, N. U., Kuti, M., Lyons, T. A. & Heymont, J. (1999). *Biochemistry*, **38**, 4681–4690.

Poulos, T. L. (2003). *Biochem. Biophys. Res. Commun.* **312**, 35–39.

Rieske, J. S., MacLennan, D. H. & Coleman, R. (1964). *Biochem. Biophys. Res. Commun.* **15**, 338–344.

Sainz, G., Jakoncic, J., Sieker, L. C., Stojanoff, V., Sanishvili, N., Asso, M., Bertrand, P., Armengaud, J. & Jouanneau, Y. (2006). *J. Biol. Inorg. Chem.* **11**, 235–246.

Sambrook, J. & Russell, D. W. (2001). *Molecular Cloning: A Laboratory Manual*, 3rd ed. New York: Cold Spring Harbor Laboratory Press.

Sauber, K., Fröhner, C., Rosenberg, G., Eberspächer, J. & Lingens, F. (1977). *Eur. J. Biochem.* **74**, 89–97.

Senda, M., Kishigami, S., Kimura, S., Fukuda, M., Ishida, T. & Senda, T. (2007). *J. Mol. Biol.* **373**, 382–400.

Sevrioukova, I. F., Garcia, C., Li, H., Bhaskar, B. & Poulos, T. L. (2003). *J. Mol. Biol.* **333**, 377–392.

Shintani, M., Urata, M., Inoue, K., Eto, K., Habe, H., Omori, T., Yamane, H. & Nojiri, H. (2007). *J. Bacteriol.* **189**, 2007–2020.

Smith, N., Mayhew, M., Holden, M. J., Kelly, H., Robinson, H., Heroux, A., Vilker, V. L. & Gallagher, D. T. (2004). *Acta Cryst.* D**60**, 816–822.

Tagawa, K. & Arnon, D. I. (1962). *Nature (London)*, **195**, 537–543.

Urata, M., Uchimura, H., Noguchi, H., Sakaguchi, T., Takemura, T., Eto, K., Habe, H., Omori, T., Yamane, H. & Nojiri, H. (2006). *Appl. Environ. Microbiol.* **72**, 3206–3216.